Research Article

Thanh Quoc Chau Nguyen*, Thanh Khang Vo, Duy Toan Pham, Trong Tuan Nguyen, and Giao Huynh Dang

Optimizing ultrasound-assisted extraction process of anti-inflammatory ingredients from *Launaea sarmentosa*: A novel approach

https://doi.org/10.1515/gps-2025-0079
received April 19, 2025; accepted September 08, 2025

Abstract: *Launaea sarmentosa*, a creeping herb, is utilized in folk medicines, either alone or in combination with other herbs, to treat various inflammatory diseases. Yet, the extraction efficiency improvement for its anti-inflammatory components has never been inspected deeply. Hence, response surface methodology was first employed to optimize the parameters of the ultrasound-assisted extraction process, approaching anti-inflammatory ingredients from *Launaea sarmentosa* via nitric oxide (NO) scavenging capacity. According to the Box–Behnken design model, the optimum parameters are as follows: solvent-to-solid ratio of 20.81 $mL \cdot g^{-1}$, extraction time of 15.72 min, and temperature of 51.80°C using absolute ethanol (99.8%) at a constant frequency of 37 kHz. For such optimized conditions, the actual IC_{50} value of NO removal capacity gained 206.56 $\mu g \cdot mL^{-1}$, which agreed with the obtained model value (IC_{50}, 209.68 $\mu g \cdot mL^{-1}$). Besides, the enhanced presence of anti-inflammatory ingredients was confirmed by deactivating nuclear factor-kappa B (NF-κB) signaling, thereby suppressing NO production and pro-inflammatory cytokines in LPS-stimulated RAW264.7 macrophages. Furthermore, the initial life cycle assessment results indicated that the extraction process was environmentally friendly, with low-impact indicators on ecosystems. Lastly, these findings offer valuable insight into the anti-inflammatory extraction process of *L. sarmentosa* through a novel approach, along with its potential for "green and sustainable" industrial applications.

Keywords: anti-inflammatory, response surface methodology, *Launaea sarmentosa*, life cycle assessment, optimization

1 Introduction

In recent years, the role of natural products as a supplemental dietary for preventing and treating various diseases has become increasingly popular. Indeed, most herbs exert their significant pharmaceutical influence in the treatment of metabolic disorders and inflammation, especially cancer [1]. As a result, the pharmaceutical industry has expanded its vision into the development of medicinal plants [2]. Consumer demand for the quality of these products is also more difficult, and they are increasingly strict with their effectiveness on health. To date, most evidence of biological and pharmacological characteristics has shown the presence of high amounts of flavonoid and polyphenolic compounds [3]. As a potential source of natural products, *Launaea sarmentosa* (Willd.) Alston, known as *Sa sâm* in Vietnamese, is a nutritious vegetable or creeping herb used as folk medicine, particularly in Vietnam and other countries, to treat inflammatory diseases [4]. The presence of active components, including polyphenols, flavonoids, alkaloids, and other compounds, was confirmed to exhibit antioxidant, anti-inflammatory, and antidiabetic [4–6]. Notably, its combination with the appropriate ratios of various medicinal herbs has been established as a commercial product by local companies in Vietnam and Thailand. They were consumed as health supplements to promote blood circulation, enhance cognitive function, and relieve symptoms of polyarthritis or osteoarthritis[7]. Therefore, *L. sarmentosa* served as a promising candidate for creating pharmaceutical products, especially for inflammation treatment.

* **Corresponding author: Thanh Quoc Chau Nguyen,** Department of Chemistry, College of Natural Sciences, Can Tho University, Campus II, 3/2 Street, Ninh Kieu District, Can Tho, 900000, Vietnam, e-mail: nqcthanh@ctu.edu.vn, tel: (+84) 909 747 547
Thanh Khang Vo: Bioassay Laboratory, CTU Hi-tech Building, Can Tho University, Campus II, 3/2 Street, Ninh Kieu District, Can Tho, 900000, Vietnam
Duy Toan Pham, Trong Tuan Nguyen: Department of Health Sciences, College of Natural Sciences, Can Tho University, Campus II, 3/2 Street, Ninh Kieu District, Can Tho, 900000, Vietnam
Giao Huynh Dang: College of Engineering Technology, Can Tho University, Campus II, 3/2 Street, Ninh Kieu District, Can Tho, 900000, Vietnam

Most inflammation research highlights the essential role of nitric oxide (NO), a key signaling mediator in both physiological and pathophysiological [8]. Importantly, NO at physiological levels is required to regulate cellular function, maintain vascular homeostasis, and promote wound healing, whereas excessive or sustained NO production may promote oxidative stress and exacerbate inflammation [9]. Thus, under these circumstances, NO was confirmed as one of the causes involved in neurological diseases and cancer [10]. Specifically, quantitative fractional exhaled NO is reported as a rapid clinical test for assessing airway inflammation in asthma [11]. Indeed, dysregulation of NO production and signaling pathways is implicated in various inflammatory conditions, ranging from arthritis and asthma to neurodegenerative disorders. Additionally, several disease conditions, including sepsis and liver failure, are associated with abnormally high NO secretion, and eliminating the excess NO could lead to positive outcomes [12]. Strategies for modulating NO levels encompass distinct approaches. One approach focuses on inhibiting nitric oxide synthase (NOS), the enzyme responsible for catalyzing NO synthesis, thereby reducing NO secretion. Alternatively, a second strategy involves the direct neutralization of existing NO. This is accomplished through the use of NO scavengers, which interact with NO molecules, thereby lowering the overall concentration of NO [13,14]. Consequently, both approaches are effective for evaluating and discovering NO modulators as well as anti-inflammatory agents.

On the other hand, drug development is influenced by the amount of bioactive ingredients derived from medicinal sources, meaning that developing a performance technique for extracting highly bioactive natural compounds is most important. Several extraction techniques were applied to recover bioactive compounds from herbal medicine, such as maceration, percolation, reflux or heat-reflux extraction, Soxhlet extraction, and ultrasonic-assisted extraction [15]. However, conventional extraction procedures often consume a significant volume of organic solvent over a long period of time, and non-selective extraction leads to low yield efficiency [16]. Notably, ultrasound-assisted extraction (UAE) has been suggested due to its high efficiency, simplicity, speed, and economic suitability for the extraction of heat-sensitive active ingredients. Ultrasound waves cause acoustic cavitation and enhancement of mass transfer, leading to cell wall disruption to release compounds into the medium. Thus, it reduces energy consumption, solvent usage, and extraction time while increasing extraction yield and enhancing the quality of products [17]. Besides, the efficiency of the UAE is influenced by various factors, including extraction time, temperature, solvent-to-solid ratio, and type of solvent. These variables can impact the extraction yield, especially the variations of molecular structures from the targeted ingredients. This leads to the deterioration of desired biological properties during extraction [18]. Hence, it is essential to determine the optimal conditions of the UAE for each specific material to enhance bioactive ingredients recovery. To overcome these situations, the response surface methodology (RSM) is a potential tool for optimizing the factors that affect the extraction process. Indeed, RSM combines mathematical and statistical techniques for experimental models, analyzes the impact of various parameters as well, and screens the optimum process variables to obtain advantageous surfaces [19]. Among RSM, Box–Behnken design (BBD) is widely used and suitable for three-level optimization experiments with 2–5 independent factors, employed to optimize processes that set four variables, and gives its rational design [20].

Furthermore, based on the aforementioned hypothesis, NO levels may potentially serve as an indicator of achieving the best possible extraction conditions for maximizing anti-inflammatory compounds from medicinal herbs. Nevertheless, most studies prioritize maximizing polyphenol and flavonoid concentrations via the extraction process. This approach is applied by the desire to enhance the antioxidant capacity and amplify its anti-inflammatory properties [2,21]. More recent investigations have also started incorporating alternative strategies into the optimization process. Specifically, these studies have begun to utilize the principles of protein denaturation and the inhibition of cellular NO synthesis as guiding factors in determining the optimal extraction parameters [22–24]. However, no information has been reported based on NO scavenging efficiency as the primary basis for optimizing the anti-inflammatory ingredients extraction process. Thus, in this current work, the parameters for optimizing the extraction process were evaluated, given the presence of active ingredients that neutralize the NO radicals. In contrast to previous studies, this approach emphasized improving the classification of anti-inflammatory components, reducing systematic errors associated with biological testing models, cutting costs, and being more adaptable to large-scale industrial pharmaceutical production.

Another aspect to consider is that while the extraction process focuses on optimizing efficiency, it simultaneously raises environmental concerns that need to be addressed. Energy consumption, organic solvent usage, and residue chemicals/byproducts seriously impact the environment during extraction processes. This inadvertently creates CO_2 emissions, thereby exacerbating the greenhouse effect or climate change [25,26]. Therefore, adopting green

practices for extraction reduces these impacts that directly affect climate change. One of the most commonly used systematic methods for quantifying the potential environmental impacts is life cycle assessment (LCA) [27]. At the initial evaluation stages, LCA improves an optimized process by considering ecological impacts such as energy consumption, human toxicity, and climate change, ultimately fostering sustainable development [28]. This matter is still insufficiently studied in extraction processes for anti-inflammatory ingredients.

Finally, the present study aimed to optimize the parameters of UAE processes, focusing on the anti-inflammatory components from *L. sarmentosa* using RSM with a BBD. Optimal model selection was primarily based on the impact of individual factors on the extraction efficiency. Besides, this was dependent on the sensitive anti-inflammatory ingredients obtained, which were the target of this work. Furthermore, a novel approach to optimizing extraction parameters through NO scavenging capacity was applied for the first time. The superior anti-inflammatory components of the optimized extract were confirmed, in comparison with a random extract, by inactivating the NF-κB signaling pathway, thereby significantly reducing NO secretion in LPS-stimulated RAW264.7 macrophages. This suggests developing specific anti-inflammatory products rather than those formulated with polyphenols and flavonoid ingredients. Additionally, the initial LCA provided environmental impact parameters that can be utilized to regulate and improve the extraction process, ensuring sustainability at industrial levels. Hence, these findings provide a deep insight into the methodological approach for the anti-inflammatory extraction process from *L. sarmentosa* and its eco-friendliness.

2 Materials and methods

2.1 Plant materials

The stem and leaves of *L. sarmentosa* (LSm) were gathered from Ben Tre province, Vietnam (9°56′53″N 106°30′51″E), in August 2022. The specimen was identified and deposited in the Laboratory of Medicinal Chemistry at the CTU Hi-tech Building, Can Tho University, Vietnam, under biospecimen code number (VNM00082022CTU). Samples were cleaned and then naturally dried to avoid direct sunlight until a consistent weight was achieved. Afterward, they were ground into a fine powder using a Waring two-speed laboratory blender (Cole-Parmer, USA) and stored in a polyethylene bag at −20°C for further extraction.

2.2 Chemicals and reagents

All chemicals and antibodies were purchased from Sigma-Aldrich (Merck, Germany), except for the Griess-Romijn Nitrite reagent, radioimmunoprecipitation assay (RIPA) buffer, and LPS-Lipopolysaccharide (FUJIFILM-Wako, Tokyo, Japan), TRIzol reagent (Invitrogen, CA, USA), bicinchoninic acid (BCA) assay, and SuperSignal West Atto Ultimate Sensitivity substrate (Thermo Fisher Scientific, USA). Bioassay was conducted using cell counting kit-8 (CCK-8) from Dojindo Molecular Technologies (Rockville, MD, USA), Qiagen RNeasy Kit from Qiagen (Hilden, Germany), and Transcriptor Universal cDNA Master Mix and FastStart Essential DNA Green Master Mix, both obtained from Roche (Mannheim, Germany).

2.3 NO radical-scavenging activity

The nitric oxide ($NO^{\bullet}$) radical scavenging activity was evaluated according to the previous studies with slight modification [29,30]. Shortly, an equal volume of 5 mM sodium nitroprusside and various concentrations of LSm extract were mixed under exposure to light for 30 min. Then, 100 µL of the mixture was combined with 100 µL Griess-Romijn nitrite reagent. The color change from transparent to pink was attained after incubating without light at room temperature for 10 min. Absorbance at 540 nm was measured and compared to a reagent blank using a standard sodium nitrite curve ($y = 0.0034x + 0.0093$; $R^2 = 0.9992$). The IC_{50} value (half-maximal inhibitory concentration) was determined to assess the radical-scavenging efficiency, while curcumin ($y = 30.779\ln(x) - 39.421$; $R^2 = 0.996$) was compared as a positive control.

2.4 Ultrasound-assisted LSm extraction and single-factor experiments

Single-factor experiments were conducted to investigate the influence of various factors, including sample weight, solvent-to-solid ratio, solvent concentration, temperature, and extraction time, based on the efficiency of NO radical-scavenging activity. In brief, the dried powder of LSm was soaked in ethanol using an Elmasonic S100H ultrasonic water bath, operating at a frequency of 37 kHz and 150 W nominal power. To assess the impact of the sample weight, amounts ranging from 1 to 20 g were applied with the random criteria, including the solvent-to-solid ratio of 20 $mL{\cdot}g^{-1}$, ethanol concentration of 100%, and extraction conducted at 30°C for 15 min. Following this, the effect of ethanol concentration (70–100%) was evaluated, keeping

the initial weight from the previous step. Then, the optimal temperatures between 30°C and 80°C were investigated for 15 min based on the preceding conditions. Lastly, the effect of extraction time (ranging from 5 to 30 min) was assessed based on the results obtained from the previous condition. After each extraction, the supernatants were centrifuged, filtered, and then concentrated using a Rotavapor R300 (BUCHI, Flawil, Switzerland). The extract was then freeze-dried in an Infistek lyophilizer and kept at −20°C for subsequent analysis. The parameters determined from these single-factor experiments were subsequently applied in an RSM using a BDD [31,32].

2.5 BDD for UAE optimization

BBD was selected to evaluate a second-order polynomial model for UAE, focusing on optimizing NO scavenging activity (Design Expert Software v12.0.0; Stat-Ease Inc., Minneapolis, MN, USA). From the result of single-factor experiments, the response pattern was affected by three parameters, including *A*: the solvent-to-solid ratio (15–25 mL·g^{-1}), *B*: temperature (40 – 60°C), and *C*: extraction time (10–20 min); each one being investigated at three levels, labeled as −1, 0, and +1, respectively. The level of independent variables and experimental design are shown in Table 1. The model was expressed by Eq. 1 [33]:

$$Y = \beta_0 + \sum_{j=1}^{k} \beta_j + \sum_{j=1}^{k} \beta_{jj} X^2 + \sum_{i=1}^{k} \sum_{j=i+1}^{k} \beta_{ij} X_i X_j \quad (1)$$

where Y is the response value; β_0 is the constant effect; β_0, β_{jj}, and β_{ij}, are the linear, quadratic, and the interaction effect coefficients, respectively, while X_i and X_j are the independent coded variables, k = 3.

2.6 Cell viability assay

RAW 264.7 macrophage cell line (ATCC – TIB-71) was cultured in Dulbecco's modified Eagle's medium (DMEM) containing 10% (*v/v*) fetal bovine serum (FBS), supplemented with reagents including 1% (*v/v*) penicillin–streptomycin, kept in a humidified incubator of 5% CO_2 at 37°C. Afterward, cells (a density of 2×10^5 cells/well) were seeded in 96-well plates before reaching 80% cell density. Then, cells were divided into marked groups and pre-incubated with a concentration of LSm with 1 μg·mL^{-1} LPS (lipopolysaccharide from *Escherichia coli* O55:B5) or without LPS for 24 h. After removing the media, each cell group was added to a mixture of 90 μL DMEM and 10 μL CCK-8. Finally, the cell cytotoxicity was assessed at 450 nm using a microplate spectrophotometer (Epoch, BioTek, USA) [34].

Table 1: Levels of independent variables and experimental design

Factor	Independent variable	Level		
		−1	0	1
A	Solvent-to-solid ratio (mL·g^{-1})	15	20	25
B	Temperature (°C)	40	50	60
C	Extraction time (min)	10	15	20

2.7 Quantification high-performance liquid chromatography (HPLC) analysis

A Prominence-I series HPLC system (LC-2030, Shimadzu, Tokyo, Japan), equipped with a C18 analytical column (5 μm, 250 mm × 4.6 mm, Shimadzu, Tokyo, Japan) and a diode array detector (Shimadzu SPD-M20 A, Tokyo, Japan), were applied to analyze the active compounds from LSm extract, following a previously described method with minor modifications [35]. Instrument control and data analysis were performed using LabSolution software (version 5.90). Specifically, the dried extract was dissolved in methanol to a 1 mg·mL^{-1} concentration and, subsequently, filtered through a 0.45 μm nylon syringe filter. The sample injection volume was set to 10 μL, with a 1.0 mL·min^{-1} flow rate at 25°C oven temperature. The mobile phase gradient was comprised of 2% acetic acid (solvent A; HPLC grade, ≥99.8%) and methanol (solvent B; HPLC grade, ≥99.8%). A gradient elution program was employed as follows: 12% of solvent B up to 10 min, subsequently changed to achieve 20%, 30%, 50%, 60%, and 70%, followed by reductions to 20% and 10% of solvent B from 20 to 80 min, with each stage maintained for 10 min. Peaks were identified by comparing the retention times and UV spectra of pure standards, including quercetin, rutin, esculetin, and luteolin-7-O-*β*-D-glucoside, as summarized in Table 4. Data were expressed as μg·g^{-1} off dried extract with three replications.

2.8 NO detection

Cells were pre-incubated in 12-well plates with varying concentrations of LSm extract, followed by washing with phosphate-buffered saline (PBS), then stimulated with 1 μg·mL^{-1} LPS (1 μg·mL^{-1}) for 24 h. Griess-Romijn nitrite reagent was used to observe the NO secretion, whereas *N*-nitro-L-arginine

methyl ester (L-NAME; 100 μM) was indicated as a positive control [34]. Subsequently, an equal volume (100 μL) of supernatant medium and Griess reagent was mixed and incubated in the dark at room temperature for 10 min. Absorbance was then measured at 540 nm using a microplate spectrophotometer and quantified against a sodium nitrite standard curve.

2.9 Detection of an inflammatory marker

Cells were seeded in six-well plates and pretreated with the indicated concentration of LSm extract. Then, cells were washed with PBS twice and stimulated in the presence/absence of LPS for 18 h. TRIzol reagent and the Qiagen RNeasy Kit were used to extract and purify total RNA, following the manufacturer's instructions, to ensure the RNA quality for downstream experiments. Finally, *iNOS*, *TNF-α*, and *IL-6* mRNA expression was evaluated using quantitative reverse transcription polymerase chain reaction (qRT-PCR), following the protocol summarized in our previous study [34]. β-Actin was used for normalization to ensure accurate and reliable qRT-PCR results. The specific details of all primers utilized in the study are presented in Table S1.

2.10 Immunofluorescence staining

For this method, cells (a density of 2×10^4 cells/well) were seeded in Nunc Lab-Tek chamber slides (Thermo Fisher Scientific, MA, USA). Then, the cell was treated with an indicated concentration of extract, either with or without LPS, for 30 min. The treatment followed established experimental protocols for assessing cellular response [36]. In sequence, rabbit anti-p65 NF-κB antibody (1:800) and Alexar-488 secondary antibody (1:1,000) were stained to detect the p65 expression, followed by 4′,6-diamidino-2-phenylindole nuclear staining for 20 min. Then, samples were observed under a fluorescence scanning microscope FV10i (Olympus, Tokyo, Japan). The results were analyzed using MetaMorph analysis software (Molecular Devices, Sunnyvale, CA, USA).

2.11 Western blotting

Cells were pretreated with an appropriate extract concentration for 24 h before LPS stimulation. Whole proteins extracted using RIPA buffer were normalized by the BCA assay. Following 10% sodium dodecyl sulfate-polyacrylamide gel electrophoresis (*v/v*) separation, proteins were transferred to polyvinylidene difluoride membranes, blocked with OneStep Blocker (Bio-Helix, Taiwan) for 1 h, and incubated with anti-phospho-p65 primary antibodies. Protein bands were visualized using SuperSignal West Atto Ultimate Sensitivity substrate. Band intensities were quantified by ImageJ analysis software (National Institute of Health, Maryland, USA) and normalized to β-actin.

2.12 Green assessment impact

In this work, Ecochain Mobius (Ecochain Technologies B.V., Amsterdam, Netherlands), a platform designed to conduct LCA, examined the environmental impact of the extraction process [37]. The platform integrates Ecoinvent v3.9.1, a comprehensive database, compliant with ISO 14044 standards [38]. This integration allows for a structured and reliable approach to conducting LCA, ensuring accuracy and compliance in the environmental impact analysis. The Ecochain Mobius platform has been certified by the International Organization for Standardization (ISO), specifically ISO 9001:2015 for quality management and ISO 27001:2017 for information security management. In this work, the function unit was 1 g of initial raw materials for applying the LCA. The system boundary. The system boundary encompassed LSm pretreatment (i.e., electricity consumption), solvent and extraction process (Figure 1). Herein, the LCA gate-to-gate approach was employed to assess these environmental impacts of the extraction process at the lab scale. The relevant input variables for evaluating the extraction process included electrical energy consumption, solvent usage, and waste generation. From this, a streamlined LCA was carried out, covering 25 different environmental impact categories, to evaluate the broader ecological effects of the process. This suggests an overview of the method and points out the essential modifications that should be implemented in order to achieve sustainable development. The current study is focused on the UAE method, which has been extensively applied to enhance the yield of bioactive ingredients extracted from plant materials or agri-by-products [39]. Moreover, rather than using organic or toxic solvents, the UAE utilizes food-grade solvents like water or ethanol to disrupt the vegetal matrix [40]. Additionally, most studies confirmed that the UAE became the eco-friendliest option, enabling a substantial reduction in energy consumption (e.g., electricity consumption) and environmental impacts (e.g., climate change

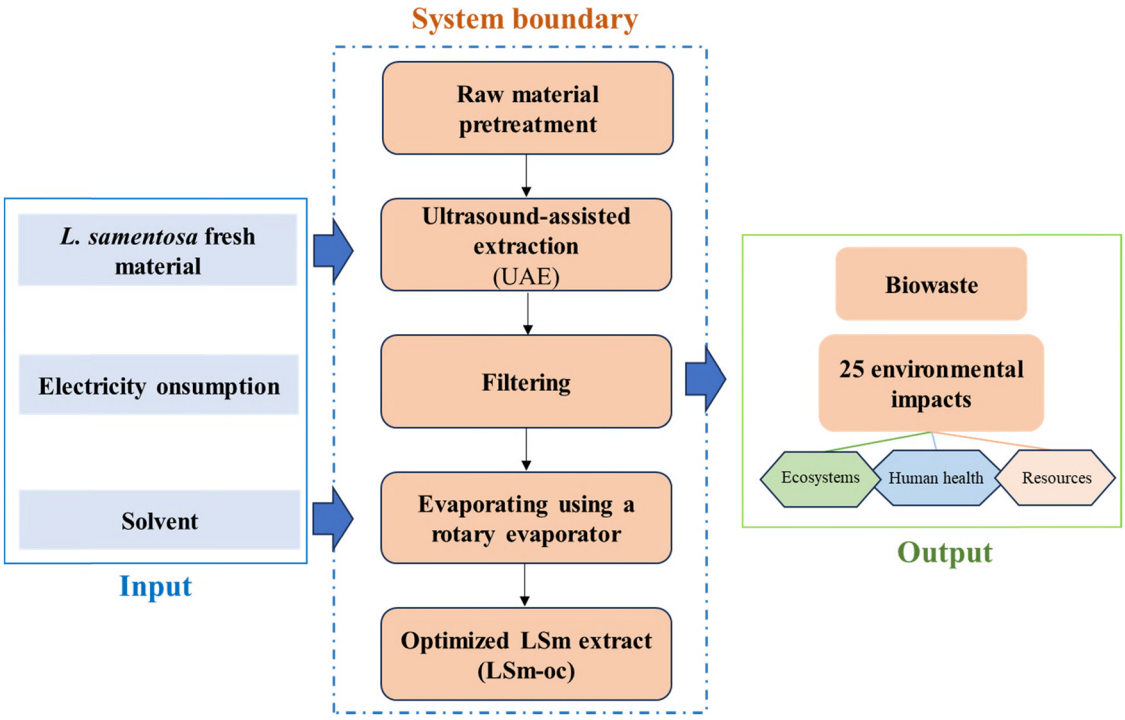

Figure 1: A schematic framework of anti-inflammatory ingredients extracted from *L. sarmentosa* using an ultrasound-assisted method (per function unit of 1 g initial raw material).

and human carcinogenic toxicity) compared to other methods [39,41,42]. Furthermore, as mentioned above, the FDA approves ethanol for specific uses in food products that meet the criteria of "Generally Recognized as Safe" (GRAS). This confirmed the safe solvent level in production, signifying low risk to health and the environment. Hence, the selected extraction technology and solvent were well-suited to minimize environmental impacts, aligning with the sustainable industrial development trend. As shown in Figure 1, the detailed flowchart of the extraction process was compiled and characterized, including materials input, energy consumption for extraction, and solvent. However, at the lab scale, plant materials' by-product was disregarded due to their being produced as biowaste. The subsequent drying, transport, residue disposal, and sale processes were not considered. Due to the small volume of solvent used, the reuse was not considered in this work. Nevertheless, while beneficial, solvent reuse typically requires a regeneration or recovery process (addition of energy input, etc.), which should be a concern on a larger scale. Therefore, electricity and solvent consumption, the main factors, were analyzed using LCA with the Environmental Footprint 3.1 methodology (EF 3.1 Method), followed by a database from Ecoinvent v3.9.1 from the Ecochain Mobius platform. Another issue is that the moisture content and scale-up mass of raw materials for industrial applications significantly impact energy consumption. High moisture or larger mass samples often need drying for initial processing, typically at 40–55°C, which consumes high electricity [39]. However, in the present work, a naturally dried sample that avoids direct sunlight was applied, and it did not affect the LCA model. Regarding the impact allocation methods, in this work, Ecochain Mobius LCA software was used, and Mobius itself did not automate allocation. Nevertheless, the physical allocation (mass, volume, energy usage) was manually applied by dividing environmental burdens based on quantifiable physical properties. Besides, scalability is reasonable when processes are linear (energy/material usage per unit is constant), no threshold effects exist (e.g., same machinery, same efficiency at small or large scales), and market effects are ignored (price elasticity, supply chain shifts).

2.13 Statistical analysis

Data was evaluated by one-way analysis of variance (ANOVA) with GraphPad Prism Software v8.0.1 (GraphPad Software Inc., San Diego, CA, USA), represented as mean ± SD of triplicate (whereas $p < 0.05$ indicated a statistically significant difference).

3 Results and discussion

3.1 Impact of individual factorst

3.1.1 Effect of sample weight

First, while maintaining all other factors constant, the weight of raw materials was varied across a range from 1 to 20 g to investigate its impact. The raw materials were derived from a blend of various components, particularly the stems and leaves of LSm. Therefore, it was crucial to consider the uniformity of the chemical composition in the extract concerning the effectiveness of its biological activity [43,44]. On the other hand, bioactivity is impacted by the inconsistency in the material's composition throughout its mass, which may complicate the creation of accurate models for large-scale industrial applications [45]. As depicted in Figure 2a, the NO scavenging activity efficiency did not vary significantly, even as the sample weight increased. This indicated that the weight of raw material did not affect the anti-inflammatory activity, likely due to the uniformity of the main active ingredients. Thus, the sample weight was set at 1 g for subsequent investigations.

3.1.2 Effect of the solvent-to-solid ratio

For the solvent-to-solid ratio, the IC_{50} initially decreased from 5 to 20 $mL \cdot g^{-1}$, which started to rise again at higher ratios (Figure 2b). This trend indicated that a ratio of 20 $mL \cdot g^{-1}$ was the most effective, reaching an IC_{50} value of 405.39 ± 1.40 $\mu g \cdot mL^{-1}$. This could be partly explained by the mass transfer and differences in solubility of active compounds at higher ratio values [46]. Increasing the solvent volume promoted better mass transfer by creating a larger concentration gradient and improving the interaction between the solvent and solute [47]. Nevertheless, the over-solvent volume could quickly reach the mass transfer equilibrium, leading to the presence of inactive ingredients and creating a complex called antagonism [14]. This effect was consistent with the previous observations [48]. Similar patterns occurred when the extraction efficiency of flavonoid compounds from *Rhus typhina* L. peaked at 30 $mL \cdot g^{-1}$

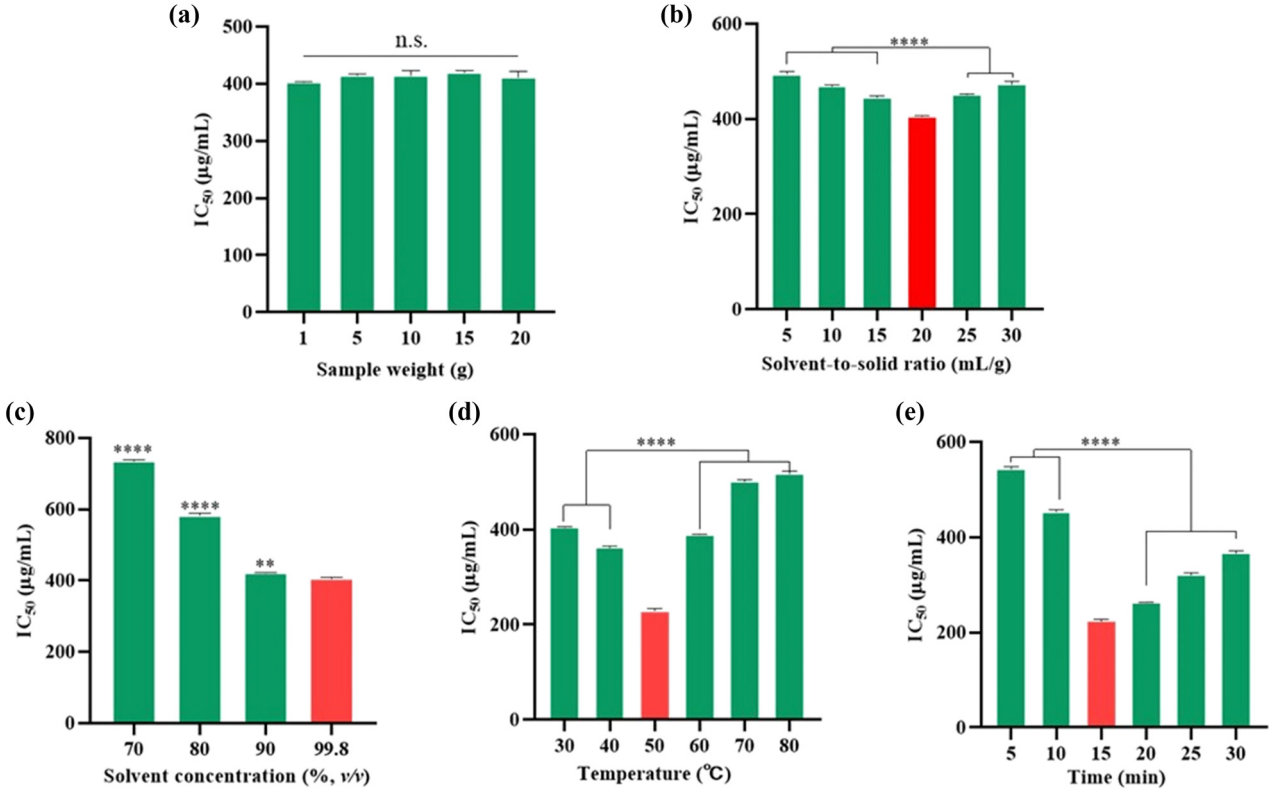

Figure 2: Effect of single factors on the NO scavenging efficiency of LSm extract. (a) Sample weight impact; (b) solvent-to-solid ratio impact; (c) solvent concentration impact; (d) temperature impact; and (e) time impact. Values were expressed as mean ± SD (n = 3), compared using one-way ANOVA with Tukey test; n.s.: not statistically significant; **p < 0.01, ****p < 0.0001.

and then sharply declined once the ratio was increased to 40 mL·g^{-1}. The solvent-to-solid ratio critically influences extraction efficiency, as well as an essential parameter that is carefully considered [49]. Excessively high ratios elevate the payment cost of the extraction process. In contrast, the low ratios may reduce the extraction quantity due to mass transfer and solubility. Therefore, an appropriate solvent-to-solid ratio was selected at 20 mL·g^{-1}.

3.1.3 Effect of the solvent concentration

To further evaluate the effect of solvent concentration on the NO removal efficiency, a volume percentage of ethanol and water was investigated, holding other parameters constant. For this, increased solvent polarity correlated with the reduction of NO removal activity in comparison with the solvent absolute (Figure 2c). It is important to note that most polyphenolic, flavonoids, or hydrolyzable tannins exhibit a stronger affinity for intermediate polar solvents [50]. Besides, according to the "like dissolves like" principle, the polarity of the solvent is similar to the solute's polarity, leading to enhanced speed and efficiency of active ingredients extraction [51]. Thus, alcohols such as ethanol or methanol are common solvents used for phytochemical extraction processes. However, ethanol is more popular than methanol and was chosen in this study due to its safety and friendly environment. Moreover, polyphenolic compounds with a large molecular weight were confirmed, rather than flavonoids with a low molecular weight [52]. As the polarity of the solvent is enhanced, these compounds disperse more easily, leading to reduced anti-inflammatory activity, whereas active ingredients typically have weak to moderate molecular weight and polarity [53,54]. As a result, 99.8% ethanol was chosen for further investigation.

3.1.4 Effect of temperature

Temperature is also a significant factor influencing the extraction process [55]. As seen in Figure 2d, increasing the temperature up to 50°C enhanced the NO scavenging efficiency, reaching the highest IC_{50} value at 229.41 ± 4.85 μg·mL^{-1}. Due to increased diffusivity, solvent molecule movement, and compound solubility improved with the rise of temperature, thereby dramatically affecting the release of active ingredients from LSm. However, at temperatures exceeding 50°C, the decomposition of these components may lead to a reduction of NO scavenging [55]. Consistent with a previous study, the extraction efficiency and biological activity significantly decreased over 70°C [56,57]. Therefore, 50°C was the most suitable temperature for this investigation.

3.1.5 Effect of time

To achieve the highest extraction efficiency and balance cost savings, extraction time is an important factor of concern. As shown in Figure 2e, the IC_{50} value steadily reduced with the rise of time, with the highest efficiency at 224.32 ± 3.37 μg·mL^{-1} after 15 min. Beyond this time, the NO scavenging yield started to decline. This behavior was due to the presence of inactive ingredients extracted or the degradation of active compounds by prolonged exposure to heat and ultrasonic waves, similar to the solvent-to-solid ratio factors above [58,59]. Lastly, a period of 15 min was selected to complete a single-factor investigation.

3.2 Optimization procedure and model fitting

According to the initial investigation of single factors, three influencing factors (i.e., the solvent-to-solid ratio from 5 to 30 mL·g^{-1}, temperature from 30°C to 80°C, and extraction time from 5 to 30 min) have directly impacted the extraction process based on NO removal efficiency. Therefore, to optimize the extraction process, the Box–Behnken matrix design with three corresponding independent variables (i.e., A, B, and C, respectively) and the results concerning the IC_{50} value of NO removal efficiency were applied in this study, as presented in Table 1. The experimental design consisted of 17 experiments, with 5 central points that exhibited the highest NO scavenging activity (Table 2). All experiments were repeated with at least three replications and were in randomized order. Particularly, the highest efficiency was observed in condition number 17 (204.71 ± 12.67 μg·mL^{-1}), while condition number 6 exhibited the lowest activity, reaching 328.58 ± 3.00 (μg·mL^{-1}). The central point was consistently marked from conditions 13 to 17, with variables A (20 mL·g^{-1}), B (50°C), and C (15 min).

Response values were estimated from experimental results using polynomial regression via the least squares method [60]. The following second-order polynomial equation describes each response based on the IC_{50} value in terms of coded factors as follows, Eq. 2:

$$IC_{50} = 211.7 - 11.39A - 6.17B - 7.62C - 29.78AB + 15.66AC - 19.4BC + 44.91A^2 + 38.33B^2 + 29.83C^2 \quad (2)$$

Table 2: Box–Behnken matrix design with coded three independent variables and IC_{50} value of NO removal efficiency from LSm

No.	Single factors			IC_{50} (μg·mL^{-1})	
	Solvent-to-solid ratio (*A*, mL·g^{-1})	Temperature (*B*, °C)	Extraction time (*C*, min)	Actual value	Predicted value
1	25	50	10	263.34^{rs} ± 8.52	267.01
2	15	60	15	320.86^{pq} ± 20.19	329.54
3	20	60	10	313.18^{noq} ± 17.26	300.72
4	15	40	15	291.52^{lmo} ± 0.33	282.75
5	15	50	20	278.23^{jkms} ± 1.00	274.56
6	25	40	15	328.58^{hioq} ± 3.00	319.50
7	20	60	20	252.08^{fgks} ± 1.72	246.67
8	25	60	15	238.81^{degs} ± 1.53	247.60
9	20	40	10	268.85^{bgkms} ± 5.71	274.26
10	15	50	10	317.73^{cimoq} ± 8.77	321.12
11	25	50	20	286.47^{bkmos} ± 7.03	283.08
12	20	40	20	285.36^{bkms} ± 6.02	297.83
13	20	50	15	214.25^{ae} ± 7.43	211.70
14	20	50	15	214.05^{ae} ± 6.33	211.70
15	20	50	15	208.03^{a} ± 9.47	211.70
16	20	50	15	217.47^{ae} ± 3.78	211.70
17	20	50	15	204.71^{a} ± 12.67	211.70

Distinct alphabet letters in the last column indicate significant value differences ($p < 0.05$). The mean ± S.D. was compared using the Tukey test ($n = 3$).

Statistical analysis (ANOVA), according to Design Expert 12.0 software, was conducted to evaluate the optimization model (Table 3). The results indicated that all regression models were highly significant ($p \leq 0.01$), and no evidence exhibited a lack of fit at the 5% significance level [61]. The regression equation formed a quadratic function with an *F*-value of 78.98, demonstrating a robust correlation with statistical variance analysis. The *p*-value was less than 0.001, implying a 0.01% probability of noise leading to the above significant *F* value. Consistent with previous studies, the model's lack of fit ($p = 0.1337$) was not substantial in terms of statistics (*p*-value >0.05), indicating that model errors were negligible. The strong correlation coefficient ($R^2 = 0.948$) also exceeded the commonly accepted 0.8 threshold. The response model demonstrated high reliability during evaluation, as indicated by a low coefficient of variation (CV) of 4.13%. This value is well below the acceptable threshold of 10%, confirming the stability of the model's outputs. This observation proved the practical applicability of this model with high dependability [48,62].

Response surface analysis, holding other factors at their central values, revealed the interaction affecting the NO removal efficiency of LSm. Figure 3a and b indicates that the optimal NO scavenging activity, equivalent to the IC_{50} minimal value, was achieved with the solvent-to-solid ratio of 19–21 mL·g^{-1}, approximately 15 min for extraction time. Similar trends were observed for other factors reached near their central field (Figure 3c–f). In comparison with *F*-values of the difference factor and surface curvature, the solvent-to-solid ratio exerted the greatest impact on the extraction rate, followed by extraction time and temperature.

Last but not least, Figure 4 depicts the optimal condition for the extraction procedure according to data analysis. The predicted IC_{50} value of NO removal efficiency is suggested at 209.68 μg·mL^{-1}, followed by the optimum conditions such as the solvent-to-solid ratio of 20.81 mL·g^{-1}, approximately 15.72 min at 51.80°C, and 99.8% ethanol. Remarkably, the actual data was obtained at 206.56 ± 2.80 μg·mL^{-1}, which aligned closely with the predicted data and was lower than curcumin with an IC_{50} value of 17.69 ± 0.32 μg·mL^{-1}. Besides, based on our current knowledge, there are no reports confirming the NO scavenging activity from LSm. Another similar information indicated that *Launaea procumbens* and *Launaea taraxacifolia*, the same genus *Launaea*, exerted stronger NO removal radical efficiency than LSm, reaching IC_{50} values of 59.4 ± 2.42 and 123.2 ± 1.5 μg·mL^{-1}, respectively [63,64]. As previously reported, biological activity differs largely depending on specific characteristics of the soil, the prevailing climate, the temperature, the distribution area, and the biodiversity of plant species [65].

3.3 Anti-inflammatory activity of LSm extract

3.3.1 Quantification of NO production

To confirm the anti-inflammatory activity of LSm through the optimization process, NO secretion was quantified

Table 3: Coefficient values of variables influence NO scavenging efficiency

Response source	Sum of squares	df	Mean square	*F*-value	*p*-value	Note
Block	575.13	2	287.56			
Model	85,063.47	9	9,451.50	78.98	<0.0001	**
A – Solvent-to-solid ratio	3,115.66	1	3,115.66	26.04	<0.0001	**
B – Temperature	914.71	1	914.71	7.64	0.0087	**
C – Time	1,393.75	1	1,393.75	11.65	0.0015	**
AB	10,641.81	1	10,641.81	88.93	<0.0001	**
AC	2,942.25	1	2,942.25	24.59	<0.0001	**
BC	4,518.54	1	4,518.54	37.76	<0.0001	**
A^2	25,472.69	1	25,472.69	212.87	<0.0001	**
B^2	18,561.72	1	18,561.72	155.11	<0.0001	**
C^2	11,241.25	1	11,241.25	93.94	<0.0001	**
Residual	4,666.92	39	119.66			
Lack of fit	3,758.61	27	139.21	1.84	0.1337	ns
Pure error	908.31	12	75.69			
Cor total	90,305.52	50				
R^2 = 0.948	R^2_{Adj} = 0.936	R^2_{Pre} = 0.905	CV = 4.13%		PRESS: 8,548.94	

**: significant at $p < 0.05$ and 0.01, respectively; ns: non-significant difference at $p > 0.05$; "cor total" denotes the corrected total sum of squares; CV: coefficient of variations; PRESS: predicted residual sum of squares.

under LPS-stimulated RAW264.7 macrophages. For this observation, the LSm extract was produced under optimal conditions (LSm-oc), and its part obtained from random conditions (LSm-rc) was chosen to conduct this comparison. First, an initial assessment of cell cytotoxicity was conducted to establish the concentration levels that ensure minimal toxicity and safety. As illustrated in Figure 5a, the cell viability in the presence of LSm-oc and

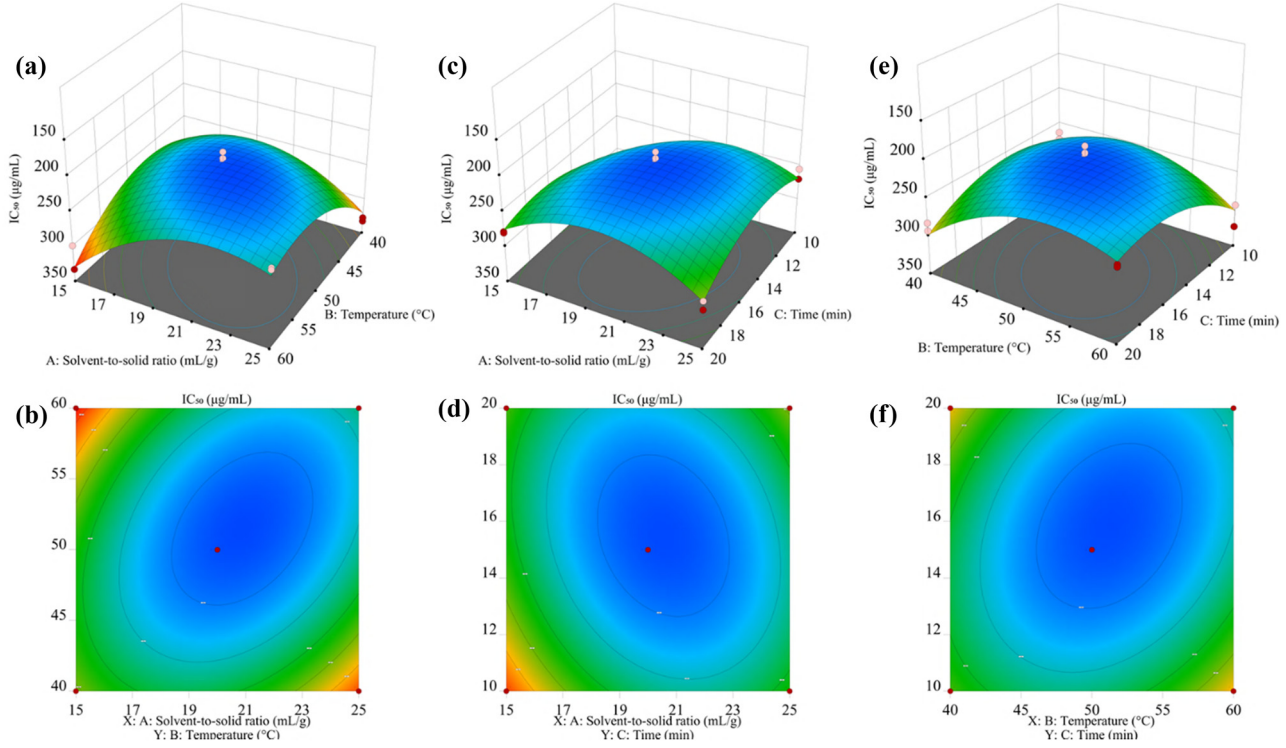

Figure 3: Response surface to NO˙ scavenging activity of LSm. (a) and (b) Response surface plots and contour plots of solvent-to-solid ratio and temperature; (c) and (d) response surface plots and contour plots of solvent-to-solid ratio and time; and (e) and (f) response surface plots and contour plots of temperature and time.

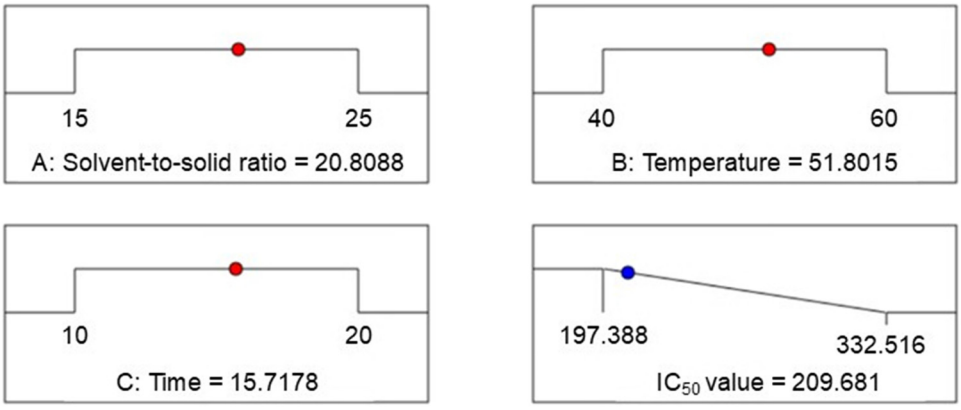

Figure 4: Predicted experimental value of the extraction process at optimized conditions.

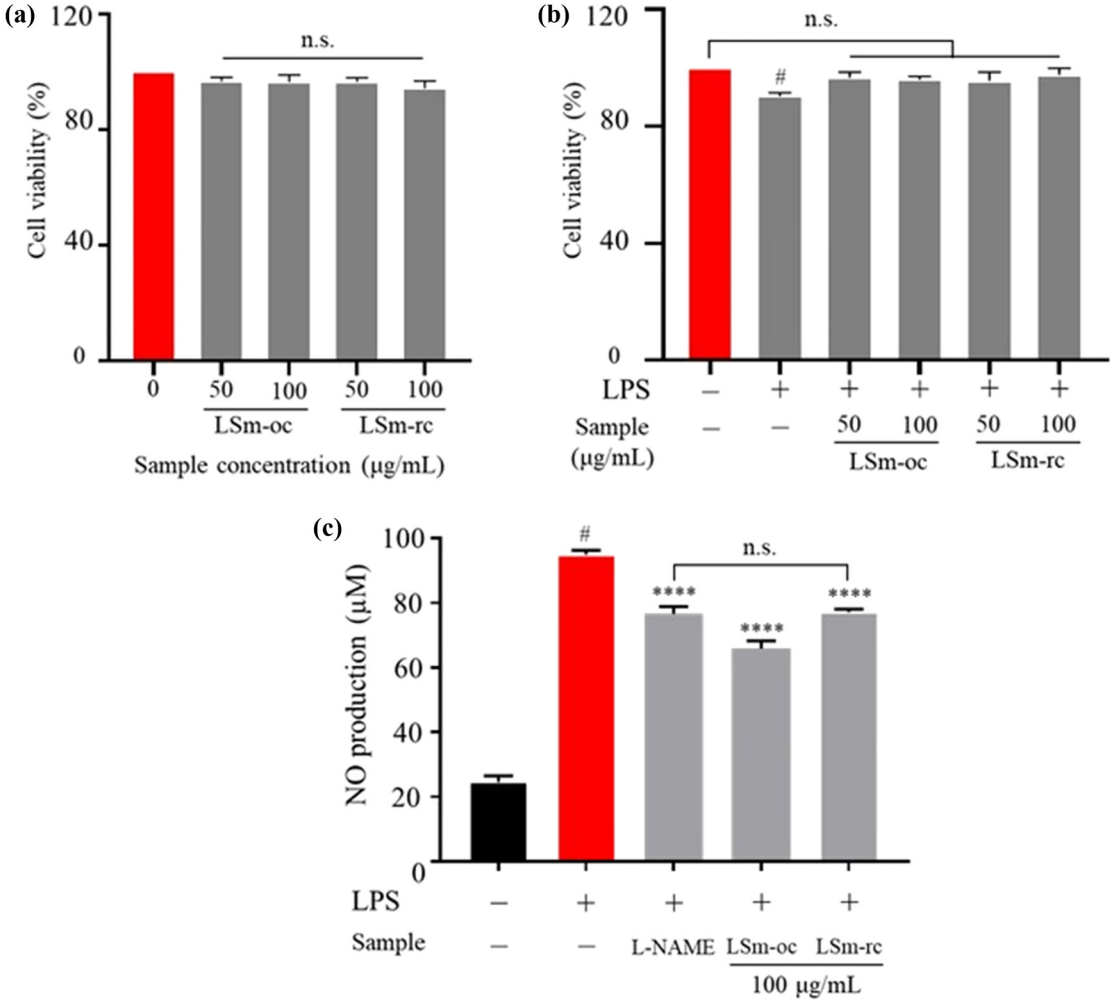

Figure 5: The effect of LSm extract on (a and b) cell viability and (c) NO production under LPS-stimulated RAW264.7 macrophages. One-way ANOVA with Sidak's multiple comparison test was applied for statistical analysis. Data were expressed as the mean ± SD ($n = 6$); n.s., not significant; $p < 0.05$ vs control without LPS; ****$p < 0.0001$ vs LPS group. LSm-oc as LSm extract under optimum conditions; LSm-rc as LSm extract under random conditions (i.e., solvent-to-solid ratio of 25 mL·g^{-1}; extraction temperature of 60°C; extraction time of 15 min).

LSm-rc was not significantly different compared to the control group. In contrast, since exposure to LPS, cell survival was reduced by over 5%, suggesting that LPS caused cell death (Figure 5b). Indeed, LPS-induced cell damage formed the phenomenon of macrophages, underscoring its impact on cell structural features [14]. This also indicated that the observation of apoptosis and pyroptosis through the morphology transformation implied abnormalities during infection occurred. Nevertheless, co-incubation with LSm-oc and LSm-rc at 5 and 10 g·mL^{-1} concentrations considerably improved cell survival in LPS-stimulated. Therefore, this issue implies that the presence of active ingredients through the extraction process may protect cells against infections by LPS.

During inflammation, macrophages, multitasking immune cells, adapt to the immune response by activating signaling cascades and then releasing pro-inflammatory cytokines [66]. As a result, NO secretion is a crucial signaling, as mentioned above, recognized when the defense mechanisms are activated against infectious pathogens [67]. Here, NO production was remarkably increased in the LPS-incubated group compared to the control and L-NAME groups. Similarly, treating LSm-oc and LSm-rc significantly suppressed the NO secretion (Figure 5c). More interestingly, at the same concentration (100 μg·mL^{-1}), LSm-oc exhibited the highest activity compared to the LSm-rc group. This aimed to re-evaluate the effectiveness of LSm-oc with inflammatory activity. Therefore, this result validated the efficiency of the optimum extraction process, emphasizing the highest concentration of anti-inflammatory components in LSm-oc.

3.3.2 Quantitative RT-PCR

Regarding the approach to inhibiting NO synthesis, the level of the inducible form of nitric oxide synthase (iNOS) was assessed using qRT-PCR. Due to NO persistent secretion under inflammatory responses, the overexpression of iNOS was initially emphasized by its role in catalyzing the creation of NO production [68]. Thus, quantitative NO secretion and iNOS levels provide an indicator of inflammation's severity and can assess pharmacological agent efficacy [14]. The mRNA expression of iNOS was up-regulated following LPS-activated RAW264.7 macrophages, whereas it was down-regulated upon pre-incubation with LSm-oc and LSm-rc incubation at 100 μg·mL^{-1} (Figure 6a). Another key marker, tumor necrosis factor-alpha (TNF-α), is a cytokine that drives inflammatory processes by activating the transcription of genes associated with inflammation and promoting cell death through indirect mechanisms. Besides, interleukin-6 (IL-6) expressed later than TNF-α, functions as a cytokine with diverse roles in acute inflammation [14]. Similar to the iNOS inhibitory level, the presence of LSm-oc strongly suppressed the mRNA expression of both TNF-α and IL-6 compared to LSm-rc (Figure 6b and c). Consistent with previous results, LSm-oc demonstrated higher efficiency than LSm-rc. This evidence proves the inhibition efficiency of LSm-oc on NO-releasing and pro-inflammatory cytokines due to the optimum active components.

3.3.3 Immunostaining detection and Western blotting

To further investigate the impact of LSm-oc and LSm-rc on inflammatory responses, an immunofluorescent analysis of NF-κB p65 was conducted to clarify this mechanism. As mentioned above, LPS stimulates the innate immune system, thereby initiating a series of complex intracellular signaling cascades. Among these signaling pathways, NF-κB signaling exerts a central role in inflammation due to promoting the release of pro-inflammatory cytokines through IκB degradation and phosphorylation of p65. In

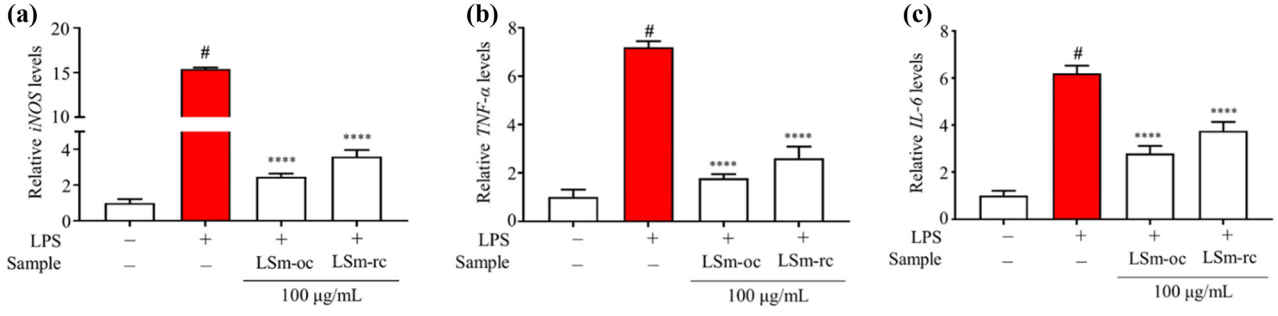

Figure 6: The pro-inflammatory and iNOS expression levels under LPS-stimulated RAW264.7 macrophages. (a) mRNA *iNOS* expression level; (b) mRNA *TNF-α* expression level; and (c) mRNA *IL-6* expression level. One-way ANOVA with Sidak's multiple comparison test was applied for statistical analysis. Data were expressed as the mean ± SD (n = 6); $^{\#}p < 0.05$ vs control without LPS; ****$p < 0.0001$ vs LPS group.

there, NF-κB subunits are sequestered in the cytoplasmic form of p50/p65 heterodimers at standard conditions, whereas infectious conditions promote their liberation and subsequently translocate into the nucleus [69]. As depicted in Figure 7a, representative micrographs of fluorescent staining demonstrated that these extracts strongly inhibited the translocation of NF-κB p65 during LPS activation. This detail has clarified the greater influence of LSm-oc compared to LSm-rc, as evidenced by the reduced intensity of p65 translocation (Figure 7b).

Furthermore, adding LSm-oc dramatically reduced the phosphorylation of p65 compared to LSm-rc, while the p-p65 protein level was significantly enhanced in LPS-stimulated macrophages (Figure 7c and d). Overall, LSm-oc strongly exerted its anti-inflammatory role by deactivating the NF-κB signaling pathway, consistent with our previous study [4]. Furthermore, this result confirmed the high presence of anti-inflammatory ingredients from the optimum extraction process.

3.4 Identification and quantification of active compounds

The presence of active compounds for both LSm-oc and LSm-rc was identified through HPLC-DAD chromatograms, as presented in Figure 8 and Figure S1. Polyphenols (i.e., luteolin-7-*O*-*β*-D-glucoside, rutin, quercetin) and coumarin (i.e., esculetin) representatives were analyzed and compared to highlight their distinguishing characteristics. These substances are popular due to their potential anti-inflammatory effects, leading to their widespread use as natural remedies [70–72]. The HPLC results revealed that LSm-oc exhibited a broader spectrum of bioactive compounds in its composition than LSm-rc (Figure 8). This indicated a more comprehensive recovery of bioactive compounds from the source material than the LSm-rc extraction. Specifically, all four compounds were identified in LSm-oc, while only luteolin-7-*O*-*β*-D-glucoside and rutin were detected in LSm-rc (Figure S1). The appearance of

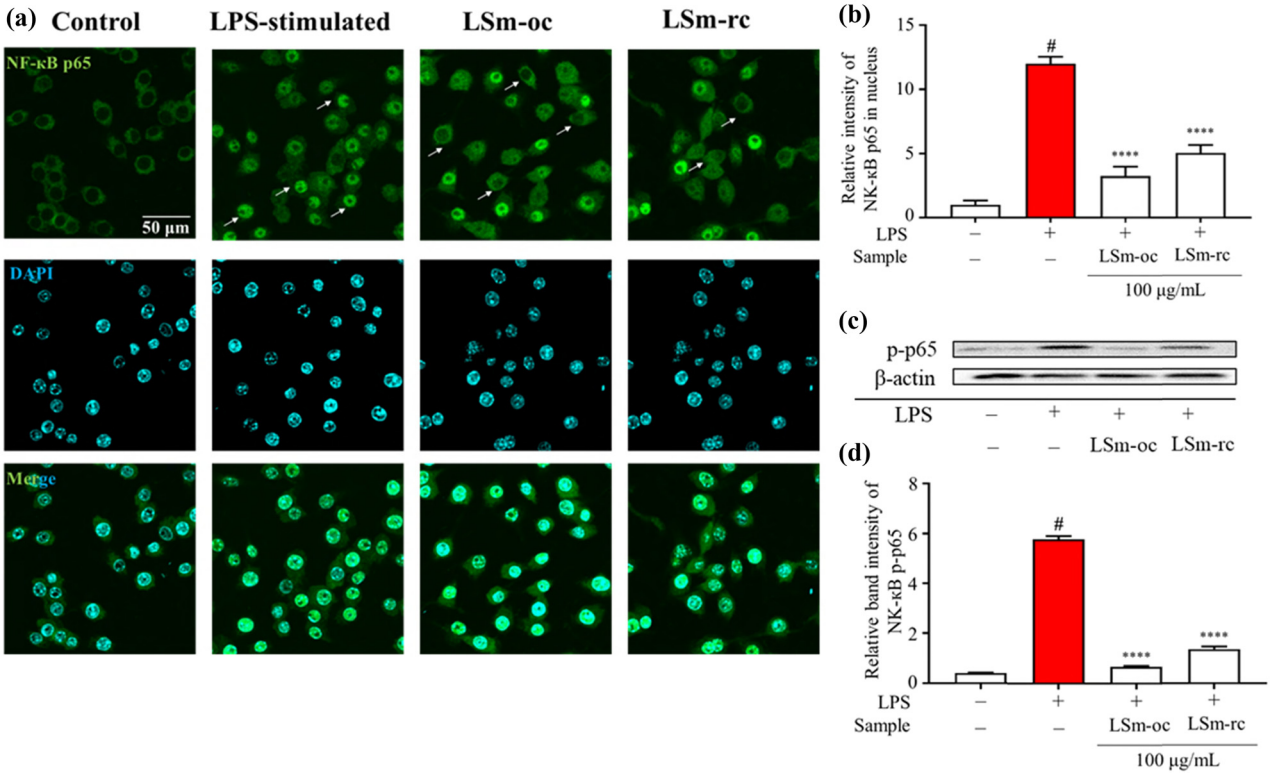

Figure 7: Inhibition of LSm-oc and LSm-rc on NF-κB p65 signaling pathway during LPS-activated RAW264.7 macrophages. (a) Immunology fluorescein-staining observation of NF-κB p65 subunit translocation; (b) nucleus fluorescent intensity was analyzed using MetaMorph software (n = 30); and (c) expression of phosphorylated-p65 following 100 μg·mL^{-1} of both extracts was analyzed by Western blot (n = 3). One-way ANOVA with Sidak's multiple comparison test was applied for statistical analysis. Data were expressed as the mean ± SD; $^{\#}p < 0.05$ vs control without LPS; ****$p < 0.0001$ vs LPS group.

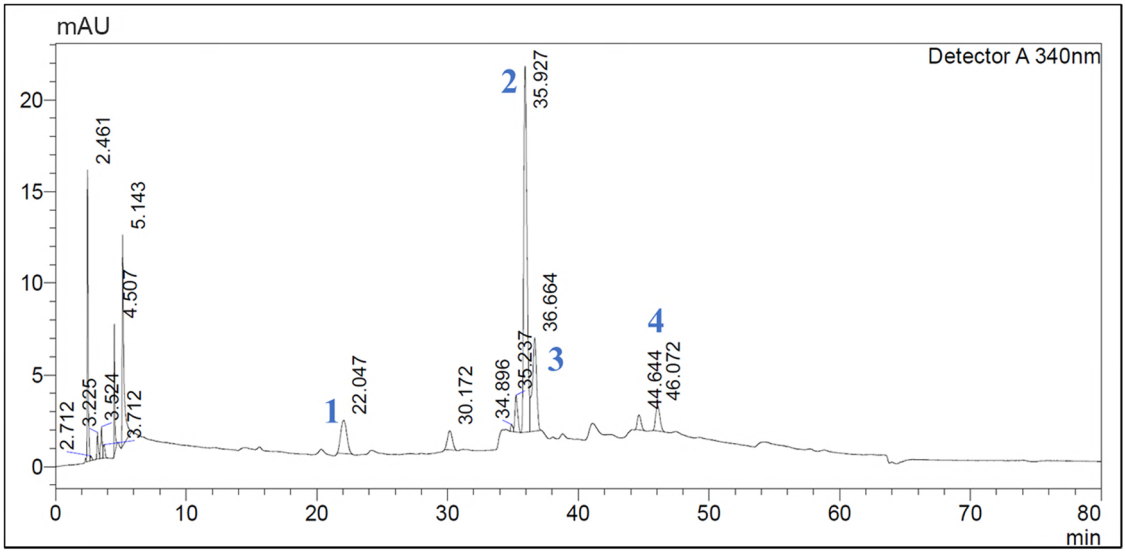

Figure 8: Representative HPLC-DAD profile of LSm optimized extract (LSm-oc). 1: esculetin; 2: luteolin-7-*O*-*β*-D-glucoside; 3: rutin; 4: quercetin.

luteolin-7-*O*-*β*-D-glucoside and rutin in LSm-oc with amounts of 14.77 and 15.83 μg·mg^{-1} dried extract, respectively, further works synergistically to enhance the extract's properties against inflammation, exerting a vital role in its overall effectiveness (Table 4). Besides, quercetin, a common compound with diverse biological effects, may have limited individual contributions at low concentrations in LSm-oc. However, its synergistic effects with other bioactive compounds could contribute to the overall efficacy.

Among the identified flavonoids, esculetin, which belongs to coumarin derivatives, appeared in LSm-oc at 2.32 μg·mg^{-1} dried extract compared to LSm-rc (Table 4). The presence of esculetin may contribute to the diversity of anti-inflammatory components from LSm-oc, consistent with our recent study [73]. Besides, other anti-inflammatory ingredients, particularly lutein, succinic acid, and 2(4-hydroxyphenyl)acetic acid, not belonging to the polyphenol group, were isolated from *L. sarmentosa* extract in our recent studies [14,74]. Remarkably, lutein, as a carotenoid with an IC_{50} value for both NO scavening activity and NO inhibition at 23.65 and 29.23 μg·mL^{-1}, respectively, served as a typical anti-inflammatory compound isolated from LSm.

In view of the findings above, this evidence offers a promising opportunity for a new approach to maximally extract anti-inflammatory agents derived from plant materials. Another issue to consider is that, despite the correlation between polyphenols or flavonoids and NO inhibitory/anti-inflammatory activity mentioned, several pieces of information indicate that NO inhibition can still be observed in plant species with low levels of their content [75,76]. In particular, good correlations between total phenolic/flavonoid contents and NO scavenging activity were obtained at 0.63 and 0.73, respectively. However, for example, *Parrotia persica* Mey leaves exert high phenolic/flavonoids as 139.2 mg gallic acid equivalent g^{-1} extract and 28.7 mg quercetin equivalent g^{-1} extract but lower NO removal activity (IC_{50}, 3.43 mg·mL^{-1}) compared to *Alcea hyrcana* Grossh leaves (IC_{50}, 0.457 mg·mL^{-1}) with

Table 4: Identification and quantification of active compounds from LSm optimized extract

No.	[a]RT (min)	Compounds	Calibration equation	[b]R^2	Concentration (μg·mg^{-1} dried extract)	
					LSm-oc	LSm-rc
1	22.047	Esculetin	y = 26,838,000 + 3,502.29	0.9995	2.32 ± 0.47	n.d.
2	35.962	Luteolin-7-*O*-*β*-D-glucoside	y = 23,097,000x − 594.84	0.9990	14.77 ± 2.32	2.63
3	36.594	Rutin	y = 7,637,610,41x – 4,856,65	0.9998	15.83 ± 1.14	4.5
4	44.638	Quercetin	y = 9,794,550x + 21,019.3	0.9999	—	n.d.

"n.d.": non-detection; "–": low intensity. [a]RT: retention time. [b]R^2 calibration graph linearity.

phenolic/flavonoids at 14.7 and 28.3 mg gallic acid and quercetin equivalent g^{-1} extract. Moreover, unfortunately, recent research implies that polyphenols, like any chemical substance, depend on the interaction, dose, and conditions, and still exert harmful effects on human health. It could possibly block iron uptake, inhibit digestive enzymes, interact with drugs, and impact hormonal balance [77]. Therefore, a strategy for developing targeted natural health products derived from herbs to replace mixed-ingredient products should be considered. Finally, these results reinforce the evidence supporting the aim of this study, emphasizing NO scavenging activity as a crucial factor for optimizing extraction.

3.5 Green assessment for the extraction process

Over the decades, rapid industrial development has posed an enormous challenge in terms of the global environment due to its severe impacts. The role of technical innovation and research activities in developing sustainable manufacturing industries addresses the balance between profitability and sustainability by adopting "greener" practices into industry processes [37]. As a result, several observations related to "eco-friendliness," such as the consumption of less energy and solvents with biodegradable properties and/or replacement technologies that ensure efficient productivity and safety, should be considered throughout the entire production cycle. A range of environmental impact variables needs to be evaluated and promptly adjusted to assess the "really green" extraction process compared to conventional extraction techniques, especially in the current context of ongoing sustainable development efforts. For this, LCA is frequently employed to assess the relative greenness or overall sustainability of new technologies and materials. This quantitative sustainability metric is highly valuable for lab research, enabling optimization at manageable control or allowing carefully refined experimental parameters [42]. This approach enables process review and is helpful for initial small-scale environmental impact assessments (e.g., raw material use, energy, solvent, and/or emissions) to inform comprehensive, larger-scale upgrades, especially the extraction process.

The growing focus on plant-based alternatives to animal products, such as functional foods, raises critical environmental questions. As these industries expand, addressing their environmental impact and ensuring sustainable practices is crucial for long-term viability and sustainable industrial development [78]. Therefore, this study aimed to address the unexplored limitations in optimizing UAE and assessing its environmental impacts for obtaining anti-inflammatory components from *L. sarmentosa*. Additionally, the initial raw material per 1 g of *L. sarmentosa* was selected as the functional unit for LCA, as mentioned above. This depends on the purpose of the LCA, focusing on input materials when the quality of the output products has been controlled, especially those related to composition and bioactivity, as reported in prior research [79].

As illustrated in Table 5, LCA results suggested several impacts, including acidification, climate change group (CC), ecotoxicity group (EC), human toxicity (HT), ionizing radiation, and ozone depletion (OD). These impact categories were frequently analyzed due to their severity on ecosystems, human health, and global warming. Regarding acidification, the transfer from CO_2 to carbonic acid (H_2CO_3) formed, reaching 90% dissolved in seawater, quickly dissociates HCO_3^-, CO_3^-, and H^+ ions are released. An increase in H^+ concentration leads to reduced pH (lower than 8.1), associated with a reduction in calcium carbonate solubility and harming marine life, especially calcifying organisms like corals and shellfish [80]. Moreover, soil acidification resulting from acid rain, as the transformation of SO_2 and NO_x composition, has significantly altered soil conditions, adversely affecting crops [81]. This indicates severe impacts on the environment that are a necessary concern through the control of acidification levels. LCA results showed that the 1.04×10^{-3} mol H^+ equiv of acidification level from the extraction process was equivalent to 7.94×10^{-4} kg SO_2 equiv and 5.9×10^{-4} kg NO_x equiv, respectively. Notably, these levels were significantly lower than in a previous study at 0.006 kg SO_2 equiv and 0.03 kg NO_x equiv [42]. Another portion of CO_2 emissions in the atmosphere contributes to the acceleration of global warming. Hence, much more attention is paid to reducing CC, as expressed by quantifying CO_2 emissions. The CC value was obtained at 1.25×10^{-1} kg CO_2 equiv, which was insignificant and 8.4-fold lower than similar criteria in flavonoid extraction from *Ginkgo biloba* leaves, reaching 1.056 kg CO_2 equiv [42]. Similarly, the freshwater and marine eutrophication (EU) at 1.07×10^{-5} kg P equiv and 1.35×10^{-4} kg N equiv were significantly lower than the values reported in this study. The EU typically attributed emissions exceeding environmental limits to freshwater or marine pollution [82]. In addition, using ethanol minimized harmful impacts on both ecosystems and human health, particularly the EC and HT, which have an approximate value of 2.64×10^{-1} CTUe (comparative toxic units ecotoxicity) and 2.53×10^{-11} CTUh (comparative toxic unit for human). Conversely, the CTUh metric can increase under the impact of organic

Table 5: Environmental impact assessment of anti-inflammatory ingredients extraction process from LSm using ultrasound-assisted method (per function unit of 1 g initial raw material)

Input			
Data	**Quantity**	**Unit**	**Ecoinvent v3.9.1 database**
Raw material	1	g	
Electricity		kWh	Market for electricity, medium voltage | electricity, medium voltage | Cutoff, *U*
Waring blender	0.03		
Ultrasonic water bath (extraction process)	0.039		
Rotary evaporator (evaporating solvent)	0.086		
Ethanol	0.01642	g	Market for ethanol, without water, in 99.7% solution state, from ethylene | ethanol, without water, in 99.7% solution state, from ethylene | Cutoff, *U*
Filter paper	0.71	g	n.a.
Biowaste	0.8	g	n.a.
Extraction yield	37%	%	n.a.
Output			
Impact categories		**Reference unit**	**Total**
Acidification		mol H^+ eq	1.04×10^{-3}
Climate change		kg CO_2 eq	1.25×10^{-1}
Climate change – biogenic		kg CO_2 eq	3.24×10^{-5}
Climate change – fossil		kg CO_2 eq	1.25×10^{-1}
Climate change – land use and LU change		kg CO_2 eq	1.13×10^{-5}
Ecotoxicity, freshwater		CTUe	2.64×10^{-1}
Ecotoxicity, freshwater – inorganics		CTUe	2.42×10^{-1}
Ecotoxicity, freshwater – organics		CTUe	2.19×10^{-1}
Eutrophication, freshwater		kg P eq	1.07×10^{-5}
Eutrophication, marine		kg N eq	1.35×10^{-4}
Eutrophication, terrestrial		mol N eq	1.50×10^{-3}
Human toxicity, cancer		CTUh	2.53×10^{-11}
Human toxicity, cancer – inorganics		CTUh	1.87×10^{-11}
Human toxicity, cancer – organics		CTUh	6.57×10^{-12}
Human toxicity, non-cancer		CTUh	9.93×10^{-10}
Human toxicity, non-cancer – inorganics		CTUh	9.62×10^{-10}
Human toxicity, non-cancer – organics		CTUh	3.11×10^{-11}
Ionising radiation		kBq U235 eq	2.61×10^{-4}
Land use		Pt	1.90×10^{-1}
Ozone depletion		kg CFC11 eq	7.42×10^{-10}
Particulate matter		Disease inc.	2.18×10^{-9}
Photochemical ozone formation		kg NMVOC eq	4.92×10^{-4}
Resource use, fossils		MJ	1.80×10
Resource use, minerals, and metals		kg Sb eq	2.14×10^{-7}
Water use		m^3-world eq	9.37×10^{-3}

Note: n.a.: non-assessment.

solvents such as benzene, etc., potentially leading to cancer or serious illnesses [83]. Finally, the OD metric, as an essential value for assessing overall environmental impacts, reflects the extent of stratospheric ozone depletion due to human chemical emissions. Based on LCA evaluation, this metric with a reference unit kg CFC11 equiv was 7.42×10^{-10}, while the allowable baseline level is 1.0 [84]. Overall, other impacts were relatively minor and did not pose any

harmful effects on the environment. These results contributed to the initial assessment of the extraction process to reduce harmful environmental impacts and minimize unnecessary costs.

4 Conclusions

For the first time, the present work suggested the optimal conditions of UAE processes, approaching anti-inflammatory components from *L. sarmentosa* via NO scavenging activity. RSM applied revealed the optimum parameters, including the solvent-to-solid ratio of 20.81 $mL \cdot g^{-1}$, the extraction time of 15.72 min, the temperature of 51.80°C, and absolute ethanol (99.8%), resulting in an IC_{50} prediction value of 209.68 and 206.56 $g \cdot mL^{-1}$ for the actual experiment, respectively. Furthermore, consistent with our previous study, the higher presence of anti-inflammatory ingredients from an optimized extract was confirmed by significantly suppressing NO production and pro-inflammatory cytokines related to blocking the NF-κB signaling pathway in LPS-activated macrophages. Besides, the initial LCA results demonstrated that the extraction process was environmentally friendly with low-impact indicators on ecosystems. Taken together, these findings offer valuable insight into the anti-inflammatory extraction process of *L. sarmentosa* through a novel approach, along with its sustainability related to the environment.

Acknowledgment: We sincerely thank Prof. Kaeko Kamei from the Institute of Technology, Kyoto, Japan, for supporting us in conducting experiments.

Funding information: This research was supported by the Ministry of Education and Training, number code: B2023-TCT-21.

Author contributions: Conceptualization: T.Q.C.N.; methodology: T.Q.C.N. and T.K.V; investigation: T.Q.C.N., T.K.V., D.T.P., T.T.N., and G.H.D.; data curation: T.Q.C.N., T.K.V., D.T.P., T.T.N., and G.H.D.; validation: T.Q.C.N. and T.K.V.; project administration: T.Q.C.N.; resource: T.Q.C.N.; writing-original draft: T.Q.C.N. and T.K.V; writing – review and editing: T.Q.C.N., T.K.V., D.T.P., T.T.N., and G.H.D. All authors have read and approved the published manuscript.

Conflict of interest: The authors state no conflicts of interest.

Data availability statement: All data generated or analysed during this study are included in this published article (and its supplementary information files).

References

[1] Nasim N, Sandeep IS, Mohanty S. Plant-derived natural products for drug discovery: Current approaches and prospects. Nucl: Int J Cytol Allied Top. 2022;65:399–411. doi: 10.1007/S13237-022-00405-3.

[2] Nekkaa A, Benaissa A, Lalaouna AED, Mutelet F, Canabady-Rochelle L. Optimization of the extraction process of bioactive compounds from Rhamnus alaternus leaves using Box-Behnken experimental design. J Appl Res Med Aromat Plants. 2021;25:100345. doi: 10.1016/J.JARMAP.2021.100345.

[3] Tungmunnithum D, Thongboonyou A, Pholboon A, Yangsabai A. Flavonoids and other phenolic compounds from medicinal plants for pharmaceutical and medical aspects: An overview. Medicines (Basel, Switzerland). 2018;5:93. doi: 10.3390/medicines5030093.

[4] Nguyen TQC, Binh TD, Kusunoki R, Pham T, Nguyen Y, Nguyen TT, et al. Effects of Launaea sarmentosa extract on lipopolysaccharide-induced inflammation via suppression of NF-κB/MAPK signaling and Nrf2 activation. Nutrients. 2020;12:2586.

[5] Hanh LH, Dung PD, Huy LD, Duong NTT, Wacharasindhu S, Phung N, et al. Chemical constituents of Launaea sarmentosa roots. Vietnam J Chem. 2020;58:637–42. doi: 10.1002/VJCH.202000057.

[6] Salih Y, Harisha CR, Shukla VJ, Acharya R. Pharmacognostical evaluation of Launaea sarmentosa (Willd.) schultz-bip.ex Kuntze root. AYU (An Int Q J Res Ayurveda). 2013;34:90. doi: 10.4103/0974-8520.115439.

[7] Tran DQ, Pham AC, Nguyen TTT, Vo TC, Vu HD, Ho GT, et al. Growth, physiological, and biochemical responses of a medicinal plant launaea sarmentosa to salinity. Horticulturae. 2024;10:388. doi: HORTICULTURAE10040388">10.3390/HORTICULTURAE10040388.

[8] Sharma JN, Al-Omran A, Parvathy SS. Role of nitric oxide in inflammatory diseases. Inflammopharmacology. 2007;15:252–9. doi: 10.1007/s10787-007-0013-x.

[9] Kim ME, Lee JS. Advances in the regulation of inflammatory mediators in nitric oxide synthase: Implications for disease modulation and therapeutic approaches. Int J Mol Sci. 2025;26:1204. doi: 10.3390/IJMS26031204.

[10] Andrabi SM, Sharma NS, Karan A, Shahriar S, Cordon B, Ma B, et al. Nitric oxide: Physiological functions, delivery, and biomedical applications. Adv Sci (Weinheim, Baden-Wurttemberg, Ger). 2023;10:2303259. doi: 10.1002/ADVS.202303259.

[11] Sandrini A, Taylor DR, Thomas PS, Yates DH. Fractional exhaled nitric oxide in asthma: An update. Respirology. 2010;15:57–70. doi: 10.1111/J.1440-1843.2009.01616.X.

[12] Shah V, Lyford G, Gores G, Farrugia G. Nitric oxide in gastrointestinal health and disease. Gastroenterology. 2004;126:903–13. doi: 10.1053/J.GASTRO.2003.11.046.

[13] Ebrahimzadeh MA, Nabavi SF, Nabavi SM, Pourmorad F. Nitric oxide radical scavenging potential of some Elburz medicinal plants. Afr J Biotechnol. 2010;9:5212–7.

[14] Nguyen TQC, Hong TT, Khang VT, Nhu Y HT, Pham DT, Giao DH, et al. Anti-inflammatory constituents isolated from Launaea sarmentosa against infection by LPS-stimulated macrophages. Rec Nat Prod. 2024;18:663–73. doi: 10.25135/RNP.487.2410.3343.
[15] Martins R, Barbosa A, Advinha B, Sales H, Pontes R, Nunes J. Green extraction techniques of bioactive compounds: A state-of-the-art review. Processes. 2023;11:2255. doi: 10.3390/PR11082255.
[16] Fan Z, Li L, Bai X, Zhang H, Liu Q, Zhang H, et al. Extraction optimization, antioxidant activity, and tyrosinase inhibitory capacity of polyphenols from Lonicera japonica. Food Sci Nutr. 2019;7:1786–94. doi: 10.1002/fsn3.1021.
[17] Maher T, Kabbashi NA, Mirghani MES, Alam MZ, Daddiouaissa D, Abdulhafiz F, et al. Optimization of ultrasound-assisted extraction of bioactive compounds from acacia seyal gum using response surface methodology and their chemical content identification by Raman, FTIR, and GC-TOFMS. Antioxidants (Basel, Switzerland). 2021;10:1612. doi: 10.3390/ANTIOX10101612.
[18] Hosseini H, Bolourian S, Yaghoubi Hamgini E, Ghanuni Mahababadi E. Optimization of heat- and ultrasound-assisted extraction of polyphenols from dried rosemary leaves using response surface methodology. J Food Process Preserv. 2018;42:e13778. doi: 10.1111/jfpp.13778.
[19] Lamidi S, Olaleye N, Bankole Y, Obalola A, Aribike E, Adigun I, et al. Applications of response surface methodology (RSM) in product design, development, and process optimization. Response Surf Methodol - Res Adv Appl IntechOpen. 2022;1–19. doi: 10.5772/INTECHOPEN.106763.
[20] Aybastıer Ö, Işık E, Şahin S, Demir C. Optimization of ultrasonic-assisted extraction of antioxidant compounds from blackberry leaves using response surface methodology. Ind Crop Prod. 2013;44:558–65. doi: 10.1016/J.INDCROP.2012.09.022.
[21] Wu EY, Sun WJ, Wang Y, Zhang GY, Xu BC, Chen XG, et al. Optimization of ultrasonic-assisted extraction of total flavonoids from Abrus Cantoniensis (Abriherba) by response surface methodology and evaluation of its anti-inflammatory effect. Molecules. 2022;27:2036. doi: 10.3390/MOLECULES27072036.
[22] Nallasamy L, Swaminathan A, Krishnamoorthy D, Murugavelu GS, Selvaraj SL. Optimization of anti-inflammatory activity of Rauvolfia tetraphylla L. crude extracts using response surface methodology. Indian J Pharm Educ Res. 2024;58:s934–43. doi: 10.5530/IJPER.58.3S.94.
[23] Jang M, Jeong SW, Kim BK, Kim JC. Extraction optimization for obtaining Artemisia capillaris extract with high anti-inflammatory activity in RAW 264.7 macrophage cells. Biomed Res Int. 2015;2015:872718. doi: 10.1155/2015/872718.
[24] Aini MA, Rusmidi MH, Adzfa K, Iran N, Pardi F, Ismail A, et al. Optimization of anti-inflammatory potential of astaxanthin and tocotrienols cocktails in lipopolysaccharide (LPS) stimulating RAW 2647 macrophages. Proceedings of the International Conference on Science Technology and Social Sciences – Biology Track (ICONSTAS-BIO 2023), Advances in Biological Sciences Research. Van Godewijckstraat, Dordrecht, The Netherlands: Atlantis Press; 2024. p. 40–57. doi: 10.2991/978-94-6463-536-2_5.
[25] Larsson DG. Pollution from drug manufacturing: Review and perspectives. Philos Trans R Soc Lond Ser B, Biol Sci. 2014;369:20130571. doi: 10.1098/RSTB.2013.0571.
[26] Verlinden A, Boone L, De Soete W, Dewulf J. Environmental impacts of drug products: The effect of the selection of production sites in the supply chain. Sustain Prod Consum. 2024;52:1–11. doi: 10.1016/J.SPC.2024.10.016.
[27] Li X, Yuan Y, Li F, Shimizu N. Early-stage life cycle assessment and optimization of aqueous crude glycerol extraction and nanofiltration concentration of tomato leaf residue. ACS Sustain Chem Eng. 2024;12:2646–55. doi: 10.1021/acssuschemeng.3c06655.
[28] Curran MA. Life cycle assessment: A review of the methodology and its application to sustainability. Curr Opin Chem Eng. 2013;2:273–7. doi: 10.1016/J.COCHE.2013.02.002.
[29] Das G, Patra JK, Debnath T, Ansari A, Shin HS. Investigation of antioxidant, antibacterial, antidiabetic, and cytotoxicity potential of silver nanoparticles synthesized using the outer peel extract of Ananas comosus (L.). PLoS One. 2019;14:0220950. doi: 10.1371/journal.pone.0220950.
[30] Mahmud ZA, Bachar SC, Hasan CM, Emran TB, Qais N, Uddin MMN. Phytochemical investigations and antioxidant potential of roots of Leea macrophylla (Roxb.). BMC Res Notes. 2017;10:245. doi: 10.1186/S13104-017-2503-2.
[31] Zulkifli SA, Abd Gani SS, Zaidan UH, Halmi MIE. Optimization of total phenolic and flavonoid contents of defatted pitaya (Hylocereus polyrhizus) seed extract and its antioxidant properties. Molecules. 2020;25(4):787. doi: 10.3390/MOLECULES25040787.
[32] Wu W, Jiang S, Liu M, Tian S. Simultaneous process optimization of ultrasound-assisted extraction of polyphenols and ellagic acid from pomegranate (Punica granatum L.) flowers and its biological activities. Ultrason Sonochem. 2021;80:105833. doi: 10.1016/J.ULTSONCH.2021.105833.
[33] Biswas A, Dey S, Xiao A, Deng Y, Birhanie ZM, Roy R, et al. Ultrasound-assisted extraction (UAE) of antioxidant phenolics from Corchorus olitorius leaves: A response surface optimization. Chem Biol Technol Agric. 2023;10:64. doi: 10.1186/s40538-023-00443-2.
[34] Nguyen TQC, Duy Binh T, Pham TLA, Nguyen Y, Thi Xuan Trang D, Nguyen TT, et al. Anti-inflammatory effects of Lasia spinosa leaf extract in lipopolysaccharide-induced RAW 264.7 macrophages. Int J Mol Sci. 2020;21:3439. doi: 10.3390/ijms21103439.
[35] Adoui N, Bendif H, Haouame I, Cam D, Rebbas K, Boufahja F, et al. Unveiling the phytochemical profiling by chromatographic and spectrometric techniques and the bioactive potential of Rumex vesicarius L. Food Anal Methods. 2025;18:1465–82. doi: 10.1007/S12161-025-02796-W/TABLES/7.
[36] Chen R. Immunoflurescence (Indirect Staining) protocol for adherent cells. Bio Protoc. 2012;2:1–3.
[37] Khanna N, Wadhwa J, Pitroda A, Shah P, Schoop J, Sarıkaya M. Life cycle assessment of environmentally friendly initiatives for sustainable machining: A short review of current knowledge and a case study. Sustain Mater Technol. 2022;32:e00413. doi: 10.1016/J.SUSMAT.2022.E00413.
[38] El Chami D, Santagata R, Moretti S, Moreschi L, Del Borghi A, Gallo M. A life cycle assessment to evaluate the environmental benefits of applying the circular economy model to the fertiliser sector. Sustainability. 2023;15:15468. doi: 10.3390/SU152115468.
[39] Vauchel P, Colli C, Pradal D, Philippot M, Decossin S, Dhulster P, et al. Comparative LCA of ultrasound-assisted extraction of polyphenols from chicory grounds under different operational conditions. J Clean Prod. 2018;196:1116–23. doi: 10.1016/J.JCLEPRO.2018.06.042.
[40] Patist A, Bates D. Ultrasonic innovations in the food industry: From the laboratory to commercial production. Innovative Food Sci Emerg Technol. 2008;9:147–54. doi: 10.1016/J.IFSET.2007.07.004.
[41] Bouchez A, Vauchel P, Périno S, Dimitrov K. Multi-criteria optimization including environmental impacts of a microwave-assisted extraction of polyphenols and comparison with an

ultrasound-assisted extraction process. Foods. 2023;12:1750. doi: 10.3390/FOODS12091750.
[42] Wang X, Wei Y, Fan Z, Chen Y, Cui Z. Life cycle assessment for evaluation of novel solvents and technologies: A case study of flavonoids extraction from Ginkgo biloba leaves. Sci Total Environ. 2024;922:171319. doi: 10.1016/J.SCITOTENV.2024.171319.
[43] Siddiqui A, Chand K, Shahi NC. Effect of process parameters on extraction of pectin from sweet lime peels. J Inst Eng (India): Ser A. 2021;102:469–78. doi: 10.1007/S40030-021-00514-3/FIGURES/3.
[44] Hlatshwayo S, Thembane N, Krishna SBN, Gqaleni N, Ngcobo M. Extraction and processing of bioactive phytoconstituents from widely used South African medicinal plants for the preparation of effective traditional herbal medicine products: A narrative review. Plants (Basel, Switz). 2025;14:206. doi: 10.3390/PLANTS14020206.
[45] Hassim N, Markom M, Rosli MI, Harun S. Scale-up approach for supercritical fluid extraction with ethanol–water modified carbon dioxide on Phyllanthus niruri for safe enriched herbal extracts. Sci Rep. 2021;11:15818. doi: 10.1038/s41598-021-95222-0.
[46] Dar IH, Junaid PM, Ahmad S, Shams R, Dash KK, Shaikh AM, et al. Optimization of ultrasound-assisted extraction of Nigella sativa seed oil for enhancement of yield and antioxidant activity. Discov Appl Sci. 2024;6:104. doi: 10.1007/S42452-024-05714-7/FIGURES/4.
[47] Nekkaa A, Benaissa A, Lalaouna AED, Mutelet F, Canabady-Rochelle L. Optimization of the extraction process of bioactive compounds from Rhamnus alaternus leaves using Box-Behnken experimental design. J Appl Res Med Arom Plants. 2021;25:100345. doi: 10.1016/J.JARMAP.2021.100345.
[48] Lai J, Wang H, Wang D, Fang F, Wang F, Wu T. Ultrasonic extraction of antioxidants from Chinese Sumac (Rhus typhina L.) fruit using response surface methodology and their characterization. Molecules. 2014;19:9019–32. doi: 10.3390/MOLECULES19079019.
[49] Zheng X, Wang X, Lan Y, Shi J, Xue SJ, Liu C. Application of response surface methodology to optimize microwave-assisted extraction of silymarin from milk thistle seeds. Sep Purif Technol. 2009;70:34–40. doi: 10.1016/J.SEPPUR.2009.08.008.
[50] Chamali S, Bendaoud H, Bouajila J, Camy S, Saadaoui E, Condoret JS, et al. Optimization of accelerated solvent extraction of bioactive compounds from Eucalyptus intertexta using response surface methodology and evaluation of its phenolic composition and biological activities. J Appl Res Med Arom Plants. 2023;35:100464. doi: 10.1016/J.JARMAP.2023.100464.
[51] Zhang QW, Lin LG, Ye WC. Techniques for extraction and isolation of natural products: A comprehensive review. Chin Med. 2018;13:20. doi: 10.1186/s13020-018-0177-x.
[52] Them LT, Tuong Nguyen Dung P, Thi Nhat Trinh P, Tong Hung Q, Tuong Vi LN, Trong Tuan N, et al. Saponin polyphenol, flavonoid content and α-glucosidase inhibitory activity, antioxidant potential of launaea sarmentosa leaves grown in Ben Tre province, Vietnam. IOP Conf Ser: Mater Sci Eng. 2019;542:012036. doi: 10.1088/1757-899X/542/1/012036.
[53] Che L, Li Y, Song R, Qin C, Hao W, Wang B, et al. Anti inflammatory and anti apoptosis activity of taraxasterol in ulcerative colitis in vitro and in vivo. Exp Ther Med. 2019;18:1745–51. doi: 10.3892/ETM.2019.7736.
[54] Dang T, Zheng G, Zhang Q, Jin P, Zhang H, Su L, et al. Sesquiterpenoids with diverse carbon skeletons from the roots of Cichorium glandulosum and their anti-inflammatory activities. Fitoterapia. 2019;136:104170. doi: 10.1016/J.FITOTE.2019.104170.
[55] Silva E, Rogez H, Larondelle Y. Optimization of extraction of phenolics from Inga edulis leaves using response surface methodology. Sep Purif Technol. 2007;55:381–7. doi: 10.1016/J.SEPPUR.2007.01.008.
[56] Zheng N, Ming Y, Chu J, Yang S, Wu G, Li W, et al. Optimization of extraction process and the antioxidant activity of phenolics from sanghuangporus baumii. Molecules. 2021;26:1–14. doi: 10.3390/molecules26133850.
[57] Wang Y, Ouyang F, Teng C, Qu J. Optimization for the extraction of polyphenols from Inonotus obliquus and its antioxidation activity. Prep Biochem Biotechnol. 2021;51:852–9. doi: 10.1080/10826068.2020.1864642.
[58] Zhang H, Wang X, He D, Zou D, Zhao R, Wang H, et al. Optimization of flavonoid extraction from Xanthoceras sorbifolia bunge flowers, and the antioxidant and antibacterial capacity of the extract. Molecules. 2021;27:113. doi: 10.3390/MOLECULES27010113.
[59] Kaufmann B, Christen P. Recent extraction techniques for natural products: microwave-assisted extraction and pressurised solvent extraction. Phytochem Anal: PCA. 2002;13:105–13. doi: 10.1002/PCA.631.
[60] Khuri AI, Mukhopadhyay S. Response surface methodology. Wiley Interdiscip Rev Comput Stat. 2010;2:128–49. doi: 10.1002/WICS.73.
[61] Aliakbarian B, Fathi A, Perego P, Dehghani F. Extraction of antioxidants from winery wastes using subcritical water. J Supercrit Fluids. 2012;65:18–24. doi: 10.1016/J.SUPFLU.2012.02.022.
[62] Cui H, Lu T, Wang M, Zou X, Zhang Y, Yang X, et al. Flavonoids from Morus alba L. Leaves: Optimization of extraction by response surface methodology and comprehensive evaluation of their antioxidant, antimicrobial, and inhibition of α-amylase activities through analytical hierarchy process. Molecules. 2019;24:2398. doi: 10.3390/MOLECULES24132398.
[63] Khan RA, Khan MR, Sahreen S, Ahmed M. Assessment of flavonoids contents and in vitro antioxidant activity of Launaea procumbens. Chem Cent J. 2012;6:43. doi: 10.1186/1752-153X-6-43.
[64] Adinortey MB, Ansah C, Weremfo A, Adinortey CA, Adukpo GE, Ameyaw EO, et al. DNA damage protecting activity and antioxidant potential of Launaea taraxacifolia leaves extract. J Nat Sci Biol Med. 2018;9:6–13. doi: 10.4103/JNSBM.JNSBM_22_17.
[65] Chaachouay N, Zidane L. Plant-derived natural products: A source for drug discovery and development. Drugs Drug Candidates. 2024;3:184–207. doi: 10.3390/DDC3010011.
[66] Lendeckel U, Venz S, Wolke C. Macrophages: Shapes and functions. ChemTexts. 2022;8:12. doi: 10.1007/S40828-022-00163-4/TABLES/3.
[67] Nguyen TQC, Kim Yen H, Trong Tuan N, Thanh Men T, Duc C, Dat MH, et al. Investigation of anti-oxidative stress and anti-inflammatory constituents from sphaerocoryne affinis leaves. Rec Nat Prod. 2025;2:157–68. doi: 10.25135/RNP.502.2502.3425.
[68] Zamora R, Vodovotz Y, Billiar TR. Inducible nitric oxide synthase and inflammatory diseases. Mol Med (Cambridge, Mass). 2000;6:347–73. doi: 10.1007/BF03401781.
[69] Xie QW, Kashiwabara Y, Nathan C. Role of transcription factor NF-κB/Rel in induction of nitric oxide synthase. J Biol Chem. 1994;269:4705–8.
[70] Akash SR, Tabassum A, Aditee LM, Rahman A, Hossain MI, Hannan MA, et al. Pharmacological insight of rutin as a potential candidate against peptic ulcer. Biomed Pharmacother. 2024;177:116961. doi: 10.1016/J.BIOPHA.2024.116961.
[71] Caporali S, De Stefano A, Calabrese C, Giovannelli A, Pieri M, Savini I, et al. Anti-inflammatory and active biological properties of the plant-derived bioactive compounds luteolin and

luteolin 7-glucoside. Nutrients. 2022;14:1155. doi: 10.3390/NU14061155.
[72] Zhang W, Mulatia S, Zhang M, Huang L, Chen J, Peng Y, et al. Esculetin inhibited fever, pain, and inflammatory responses via binding to HSC70. J Ethnopharmacol. 2025;350:120022. doi: 10.1016/J.JEP.2025.120022.
[73] Nguyen TQC, Vo KT, Duong CD, Huynh TP, Ca LTT, Dang GH. Identification of anti-inflammatory components from Launaea sarmentosa using in vitro cell model. Indonesian J Chem. 2025;25:1077–86. doi: 10.22146/IJC.103167.
[74] Thanh NQC, Khang VT, Khiem NH, Hong TT, Quy HTK, Hong NT. Study on isolation of antiinflammatory compounds from n-hexane extract of Launaea sarmentosa. CTU J Sci. 2024;60:305–13.
[75] Rosero S, Del Pozo F, Simbaña W, Álvarez M, Quinteros MF, Carrillo W, et al. Polyphenols and flavonoids composition, anti-inflammatory and antioxidant properties of Andean Baccharis macrantha extracts. Plants (Basel, Switz). 2022;11:1555. doi: 10.3390/PLANTS11121555.
[76] Zaidi S, Chaher-Bazizi N, Kaddour T, Medjahed Z, Benaida-Debbache N. Optimization of ultrasound-assisted extraction of phenolic compounds from Pistacia lentiscus with the study of their antioxidant and anti-inflammatory potential. Sustain Chem Pharm. 2024;41:101678. doi: 10.1016/J.SCP.2024.101678.
[77] Duda-Chodak A, Tarko T. Possible side effects of polyphenols and their interactions with medicines. Molecules. 2023;28:2536. doi: 10.3390/MOLECULES28062536.
[78] Yuan X, Zhong M, Huang X, Hussain Z, Ren M, Xie X. Industrial production of functional foods for human health and sustainability. Foods. 2024;13:3546. doi: 10.3390/FOODS13223546.
[79] Duc CKT, Tuan NT, Linh TC, Luong HVT, Pham DT. Optimization of ultrasound-assisted extraction of Ehretia asperula leaves with antioxidant and anti-diabetic activities and assessment of the process environmental impacts. Sustain Chem Pharm. 2025;45:102039. doi: 10.1016/J.SCP.2025.102039.
[80] Bach V, Möller F, Finogenova N, Emara Y, Finkbeiner M. Characterization model to assess ocean acidification within life cycle assessment. Int J Life Cycle Assess. 2016;21:1463–72. doi: 10.1007/S11367-016-1121-X/METRICS.
[81] Yang B, Zhang H, Ke W, Jiang J, Xiao Y, Tian J, et al. Effect of soil acidification on the production of Se-Rich Tea. Plants (Basel, Switz). 2023;12:2882. doi: 10.3390/PLANTS12152882/S1.
[82] Balasuriya BTG, Ghose A, Gheewala SH, Prapaspongsa T. Assessment of eutrophication potential from fertiliser application in agricultural systems in Thailand. Sci Total Environ. 2022;833:154993. doi: 10.1016/J.SCITOTENV.2022.154993.
[83] Chiavarini M, Rosignoli P, Sorbara B, Giacchetta I, Fabiani R. Benzene exposure and lung cancer risk: A systematic review and meta-analysis of human studies. Int J Env Res Public Health. 2024;21. doi: 10.3390/IJERPH21020205.
[84] Wuebbles DJ. Ozone depletion potentials, encyclopedia of atmospheric sciences. 2nd edn. Suite, Berkeley, CA: Elsevier Inc.; 2015. p. 364–369. doi: 10.1016/B978-0-12-382225-3.00293-0.